



Research paper

BIO-INSPIRED MAGNETIC BEADS FOR ISOLATION OF SPERM FROM HETEROGENOUS SAMPLES IN FORENSIC APPLICATIONS

Fatih Inci^{a,1}, Merve Goksin Karaaslan^{a,2}, Rakhi Gupta^a, Anirudh Avadhani^a, Mehmet Giray Ogut^a, Ekin Erin Atila^a, George Duncan^b, Leonard Klevan^c, Utkan Demirci^{a,*}

^a Canary Center at Stanford for Cancer Early Detection, Bio-Acoustic MEMS in Medicine (BAMM) Laboratory, Department of Radiology, Stanford School of Medicine, Stanford University, Palo Alto, CA 94304, USA

^b School of Criminal Justice, Nova Southeastern University, Fort Lauderdale, FL 33314, USA

^c DxNow Inc., Gaithersburg, MD 20879, USA

ARTICLE INFO

Keywords:

Sialyl-Lewis^x
Magnetic beads
Bio-inspired material
Cell separation
Forensics

ABSTRACT

Rapid and efficient processing of sexual assault evidence will accelerate forensic investigation and decrease casework backlogs. The standardized protocols currently used in forensic laboratories require the continued innovation to handle the increasing number and complexity of samples being submitted to forensic labs. Here, we present a new technique leveraging the integration of a bio-inspired oligosaccharide (*i.e.*, Sialyl-Lewis^x) with magnetic beads that provides a rapid, inexpensive, and easy-to-use strategy that can potentially be adapted with current differential extraction practice in forensics labs. This platform (i) selectively captures sperm; (ii) is sensitive within the forensic cut-off; (iii) provides a cost effective solution that can be automated with existing laboratory platforms; and (iv) handles small volumes of sample (~200 μ L). This strategy can rapidly isolate sperm within 25 minutes of total processing that will prepare the extracted sample for downstream forensic analysis and ultimately help accelerate forensic investigation and reduce casework backlogs.

1. INTRODUCTION

Cell isolation methods have been widely used in many fields, including cancer research [1–3], cell therapy [4], infectious diseases [5–8], and forensic science [9,10]. Processing a small number of cells from heterogeneous mixtures have some difficulties and present biological and technical challenges. For instance, in forensic science, processing evidence samples from sexual assault kits requires the separation of the perpetrator's cells (sperm cells) from the victim's cells (epithelial cells). Predominantly, conventional differential extraction methods are implemented in forensic labs and require labor-intensive and time-consuming procedures, contributing significantly to the backlog problem. New strategies including acoustic trapping [11], antibody-based capture [9], laser microdissection [12–14], and nuclease-based approaches [15], have been also introduced to isolate sperm from forensic samples, however, the yield may be low at the end of the

process. Among these methods, instruments integrating magnetic bead-based strategies (*e.g.*, QIAGEN EZ1 Advanced) are widely used for DNA extractions. This strategy is also applied for sperm capture (before downstream analyses) in forensic labs [16,17]. Despite their utility, magnetic-based methods leveraging the antibody-type detection for sperm isolation have challenges when working with aged sperm samples due to the alterations in sperm surface receptors over time, decreasing the observed yields of sperm DNA [17]. Earlier, we showed that a bio-inspired molecule (SLeX: Sialyl-Lewis^x) integrated with a microfluidic chip platform can perform sensitive and specific isolation of sperm from heterogeneous mixtures and achieve high yields for the samples older than 15 years [18]. However, challenges remain for the integration of these highly selective molecules to carriers that can be easily integrated to the current forensic lab protocols. Briefly, our earlier work was based on the integration of SLeX molecules into a microfluidic chip that includes multiple fabrication and surface chemistry steps. To

* Corresponding author at: Canary Center at Stanford for Cancer Early Detection, Bio-Acoustic MEMS in Medicine (BAMM) Laboratory, Department of Radiology, Stanford School of Medicine, Stanford University, Palo Alto, CA 94304, USA.

E-mail address: utkan@stanford.edu (U. Demirci).

¹ Present address: UNAM-National Nanotechnology Research Center and Institute of Materials Science and Nanotechnology, Bilkent University, Ankara, 06800, Turkey.

² Present address: Department of Property Protection and Security, Taskent Vocational High School, Selcuk University, Konya, Turkey.

further advance the field, there are three main technological and methodological challenges remaining: (i) a new technology needs to isolate sperm cells specifically, resulting in a high yield; (ii) the overall method needs to be easily adapted to current forensic practices; and (iii) sample manipulation steps need to be facile, hence minimizing the requirement of skilled personnel and intensive training of current researchers at a crime laboratory. This new approach makes the isolation method more translatable to a forensics setting. To make our approach more applicable and readily available in forensic labs, we demonstrate integration into a magnetic bead-based format using a 1.5 mL volume of microcentrifuge tube, where sample manipulation steps are relatively simple for a forensic laboratory conditions. By uniquely integrating the SLeX approach with magnetic beads, we denote a new method that can be much easily integratable and scalable with high throughput downstream forensic lab processes such as a 96-well format.

Here, we demonstrate a combined strategy, where a bio-inspired material is integrated with magnetic beads to isolate sperm cells specifically (Fig. 1). In this approach, we aim to leverage the easy-adaptation feature of magnetic bead type strategies that accelerate the platform utility into the existing forensic labs' procedures, and also, benefit from the high specificity, durability, and selectivity features of SLeX molecule. The integration of bio-inspired SLeX molecules to already existing forensic lab protocols (magnetic bead-based isolation

strategy) would potentially accelerate the access and translation of these urgently needed technologies into the crime lab. By combining these two strategies, this platform specifically captures sperm cells and provides an inexpensive alternative to the current protocols. It also needs a small sample volume (~200 μ L) to process within 25 minutes of total processing for further potential downstream forensic analyses and should be adoptable to high-throughput automated procedures.

2. MATERIALS AND METHODS

2.1. Surface functionalization for magnetic beads

According to the manufacturer's directions, we initially transferred a homogenous solution of magnetic beads (575×10^6 beads) (supplied at 10 mg/mL in N,N-dimethylacetamide (DMAC), purchased from Thermo Fisher Scientific (Waltham, MA, USA)) to a microcentrifuge tube (1.5 mL) and placed the tube on a magnetic stand (the MACS Separator, purchased from Miltenyi Biotec (North Rhine-Westphalia, Germany)). The magnetic beads were then collected, and the supernatant was discarded. The ice-cold Wash Buffer A (300 μ L of 1 mM of hydrochloric acid, purchased from Sigma-Aldrich (St. Louis, MO, USA)) was applied to the tube, and vortexed gently for 15 seconds to mix homogeneously. Again, the magnetic beads were collected, and the supernatant was

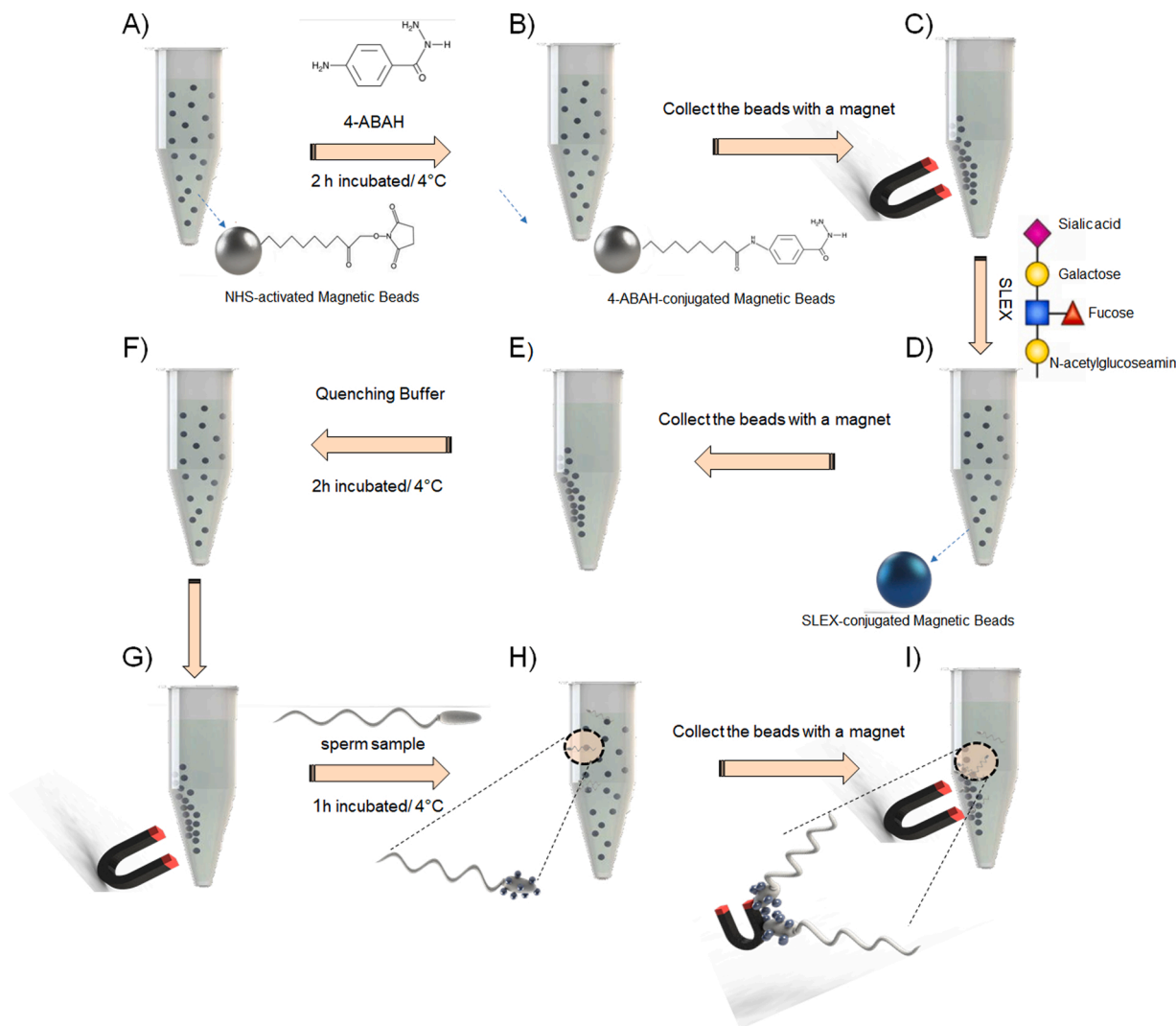


Fig. 1. Workflow and surface chemistry procedure. A-G) Magnetic beads were chemically modified using 4-ABA-H and SLeX reagents, and the process was terminated by adding the quenching buffer. H-I) Sperm cells were applied into the microcentrifuge tube, and after an incubation, the cells were collected using a magnet.

discarded. The aminobenzoic acid hydrazide (4-ABAH, purchased from Sigma-Aldrich (St. Louis, MO, USA)) (200 μ L) solution was added to form hydrazide groups on the bead surface. The stock concentration of 4-ABAH was prepared as 10 mg/mL in Dimethyl sulfoxide (DMSO) (Fisher Scientific (Hampton, NH, USA)), and the experiment concentration of 4-ABAH was tested within a range of 100 μ g/mL – 500 μ g/mL prepared with DMSO:phosphate buffered saline (PBS, Thermo Fisher Scientific (Waltham, MA, USA)) (1:1 (v:v) ratio). After adding 4-ABAH, the tube was incubated for 2 hours on a rotator at 4 °C (during the first 30 minutes, the tube was vortexed for 15 seconds every 5 minutes). At the end of the incubation period, the bead solution was placed on a magnetic stand and incubated for 30 seconds (same procedure were applied to all bead collection steps using a magnetic stand). The beads were then collected, and the supernatant was discarded. To remove any chemical residues in the tube, the magnetic beads were washed with 300 μ L of PBS and vortexed for 15 seconds. After that, we collected the beads on the magnetic stand, and applied washing steps again.

A 200 μ L of SLeX (purchased from EMD Millipore (Hayward, CA, USA)) solutions in different concentrations, ranging from 100 μ g/mL to 500 μ g/mL in PBS, were added into the tube, and the solution was allowed for an overnight incubation (16 to 20 hours) on a rotator at 4 °C (during the first 30 minutes, the tube was vortexed for 15 seconds at every 5 minutes). After the incubation period, we collected the beads using a magnetic stand, and discarded the supernatant. We added 300 μ L of PBS to the beads and vortexed the tube for 15 seconds. Again, we collected the beads on the magnetic stand, and applied the same washing steps. To alter the PBS buffer condition, we applied the same washing, vortexing, and bead collection steps with 300 μ L of deionized (DI) water. After the DI washing step, 300 μ L of Quenching Buffer (3 M of ethanolamine, pH 9.0, purchased from Sigma-Aldrich (St. Louis, MO, USA)) was added to the bead solution, and the tube was vortexed for 30 seconds. The tube was incubated for 2 hours on a rotator at 4 °C. After the incubation step, we collected the beads using a magnetic stand, and discarded the supernatant. Then, 300 μ L of ultrapure water was added to the tube, and the tube was mixed by pipetting. Finally, the beads were collected with a magnetic stand, and the supernatant was discarded.

2.2. Dynamic Light Scattering (DLS) Studies

The size distribution of N-Hydroxysuccinimide (NHS)-terminated magnetic beads were analyzed with the DLS system (Malvern Panalytical, United Kingdom). The size distribution of beads was performed in a standard DLS cuvette. We prepared a mixture containing 25 μ L of bead solution and 2975 μ L DI water, and measured this mixture in a cuvette at 25 °C.

2.3. Fourier Transformed Infrared (FTIR) Spectral Studies

The chemical structure of the NHS-activated magnetic beads and SLeX-modified NHS-activated magnetic beads were characterized using an FTIR system (PerkinElmer 283 spectrum). In this method, 4 mg of sample was pelleted with potassium bromide (KBr, purchased from Sigma-Aldrich (St. Louis, MO, USA)), and the FTIR spectra was recorded in the wave number range of 500 – 4000 cm^{-1} .

2.4. Sperm and buccal cell samples

Under an IRB protocol in-place (Stanford University IRB Number: 6208, and Protocol ID: 30538), we obtained de-identified anonymous sperm samples from Stanford Medicine, Fertility and Reproductive Health Services (Sunnyvale, CA, USA). Under the same IRB, we also obtained buccal epithelial cells from female individuals' inner cheek and collected the consent forms from the subjects. Both sperm and buccal cells were not treated with any processes, such as isolation, purification or washing, and they were used directly in the experiments.

2.5. Sperm staining and quantification

Sperm were stained with DAPI, and counted by using a hemocytometer/cell counter. Briefly, we placed 100 μ L of sperm cells into a 1.5 mL microcentrifuge tube, and centrifuged the tube for 5 minutes at 1,200 rpm. After the centrifugation, we discarded the supernatant, and added 1 mL of DAPI stain (Thermo Fisher Scientific (Waltham, MA, USA)) solution (diluted in 1:100 in PBS). We incubated the tube for 10 minutes at room temperature by covering with an aluminum foil. We again centrifuged with the same parameters, and discarded the supernatant. To remove any excessive stain moieties in the tube, we added 1 mL of PBS, centrifuged with the tube for 5 minutes at 1,200 rpm, and discarded the supernatant. We applied this washing step one more time. By adding 1 mL of PBS to the sperm cell in the tube, we completed the staining procedure. For quantification, we added 10 μ L of a DAPI-labeled sperm sample to a hemocytometer/cell counter and counted the sperm cells. To reach the corresponding sperm numbers, we serially diluted the stock sperm solution in PBS. Moreover, since counting cells with hemocytometer has difficulties for low cell numbers (1×10^3 and 10×10^3 sperm), we designed a microfluidic chip (with 20 μ L of channel volume), and counted 1×10^3 sperm/200 μ L and 10×10^3 sperm/200 μ L cells in the channels using a microscope system operated with the tiling function. In this step, we used 10 microchannels to ensure apply and count the entire sperm numbers in 200 μ L of sample. We therefore confirmed our dilutions with high sperm number using a hemocytometer and low sperm number counting on a microfluidic chip.

2.6. Sperm experiments

Before starting the sperm experiments, the sperm number in the stock solution was counted using a hemocytometer or a microfluidic chip for 1×10^3 and 10×10^3 sperm/200 μ L as described above. To reach the corresponding sperm numbers, we serially diluted the stock sperm solution in PBS. After the counting, 200 μ L of sperm were added in a tube containing SLeX-integrated magnetic beads, and sperm samples were incubated (from 10 minutes to 2 hours) on a rotator at 4 °C. The tube was then placed on a magnetic stand to collect the beads, and the supernatant and unbound sperm cells were taken into another tube. The captured sperm were washed with 300 μ L of PBS (2 times) and the tube was again placed on a magnetic stand for collecting the beads, and the supernatant was taken into another tube. Due to the high number of magnetic beads creating difficulties in counting, we quantified the unbound sperm cells in the supernatant phase using a hemocytometer/cell counter. While working with low sperm numbers (1×10^3 and 10×10^3 sperm), we used a microfluidic chip for cell quantification as detailed above. The captured sperm were calculated by subtracting the number of cells (counted in the supernatant phase and after washing steps) from the stock cell number (sperm count before capture process). The captured efficiency rate was defined as follows:

$$\text{Capture efficiency (\%)} = \frac{\text{Sperm count after capture process}}{\text{Sperm count before capture process}} \times 100$$

2.7. Vaginal epithelial cell culture

Briefly, the cryovial containing primary vaginal epithelial cells (ATCC® PCS-480-010™, purchased from ATCC (Manassas, VA, USA)) were thawed rapidly in a 37 °C water-bath. The cell suspension in the cryovial was slowly transferred to a tube containing 9 mL of medium (Vaginal Epithelial Cell Basal Medium (ATCC® PCS-480-030™, purchased from ATCC (Manassas, VA, USA)), and then, the cell suspension was centrifuged at 1,500 rpm for 3 minutes. Afterwards, the supernatant was discarded, and 1 mL of medium was applied to the pellet. After discarding the supernatant, 100 μ L of cell suspension was pipetted in cell culture dishes containing 5 mL of growth media, and the dishes were placed in a 5% CO₂ incubator at 37 °C. The dishes were checked daily

using an inverted microscope, and the cell confluence was monitored regularly. The medium was then removed from primary culture using a sterile pasteur pipet and the adhering cells were washed once with PBS. The trypsin-EDTA (purchased from Thermo Fisher Scientific (Waltham, MA, USA)) solution was added to the culture to remove the adhering cell layer. Then the dishes were placed in a 5% CO₂ incubator at 37 °C for 3 minutes. We again checked the culture using an inverted microscope to ensure the cell detached from the surface. The cell suspension was transferred to a tube containing 2 mL of culture medium. The tube was then centrifuged at 1500 rpm for 3 minutes, and the supernatant was discarded. Finally, 1 mL of medium was applied to the pellet and vaginal epithelial cells were counted on a hemocytometer.

2.8. Statistical Analysis

All data presented in this study was assessed with statistical analysis using GraphPad Prism (San Diego, CA, USA) and OriginPro (Northampton, MA, USA). Diamond-shaped Box-Whisker plots represent the 25th and 75th of percentiles; red-line indicates the median; and whiskers shows the 95th and 5th percentiles. Dots indicated each data point for the concentrations. Non-parametric Kruskal-Wallis analysis followed by Dunn's multiple comparison test was used to assess the data for 4-ABAH and SLeX concentrations. The minimum, first quartile, median, third quartile, and maximum of each concentration (4-ABAH and SLeX) were represented in Tables S1 and S2. In the evaluation of assay procedure and specificity experiments, one-way analysis of variance (ANOVA) followed by Tukey's multiple comparison test was performed to evaluate

the data for each plot. In all the figures, the statistical significance threshold was set at 0.05 ($p < 0.05$), and the data size and statistical result were stated in each figure caption.

3. RESULTS AND DISCUSSIONS

3.1. Optimizing surface modification parameters

Magnetic beads were decorated with SLeX molecules *via* two main reaction steps: (i) chemical conversion from NHS esters to hydrazide groups and (ii) immobilization of SLeX molecule on the bead surface. We initially optimized the first step by evaluating different concentrations of 4-ABAH molecules from 100 µg/mL to 500 µg/mL over sperm capture efficiency while keeping the SLeX concentration (250 µg/mL), sperm number applied (1.5×10^6 cells in 200 µL of sample), and incubation time (60 minutes) constant (Fig. 2A). In this concentration range, we observed sperm capture efficiencies as $74.3 \pm 5.4\%$ for 100 µg/mL of 4-ABAH coupling reagent, $71.8 \pm 2.4\%$ for 250 µg/mL of 4-ABAH, and $73.7 \pm 8.5\%$ for 500 µg/mL of 4-ABAH. According to the statistical assessments, there was no statistical difference between all the concentrations ($n = 3-6$, $p > 0.05$) (Fig. 2A and Table S1), and we therefore continued to further experiments with 100 µg/mL of 4-ABAH concentration.

At the next step, we assessed the effect of multiple SLeX concentrations (100 µg/mL to 500 µg/mL) for sperm capture efficiency, keeping the 4-ABAH concentration (100 µg/mL), sperm number (1.5×10^6 cells in 200 µL of sample), and incubation time (60 minutes) constant

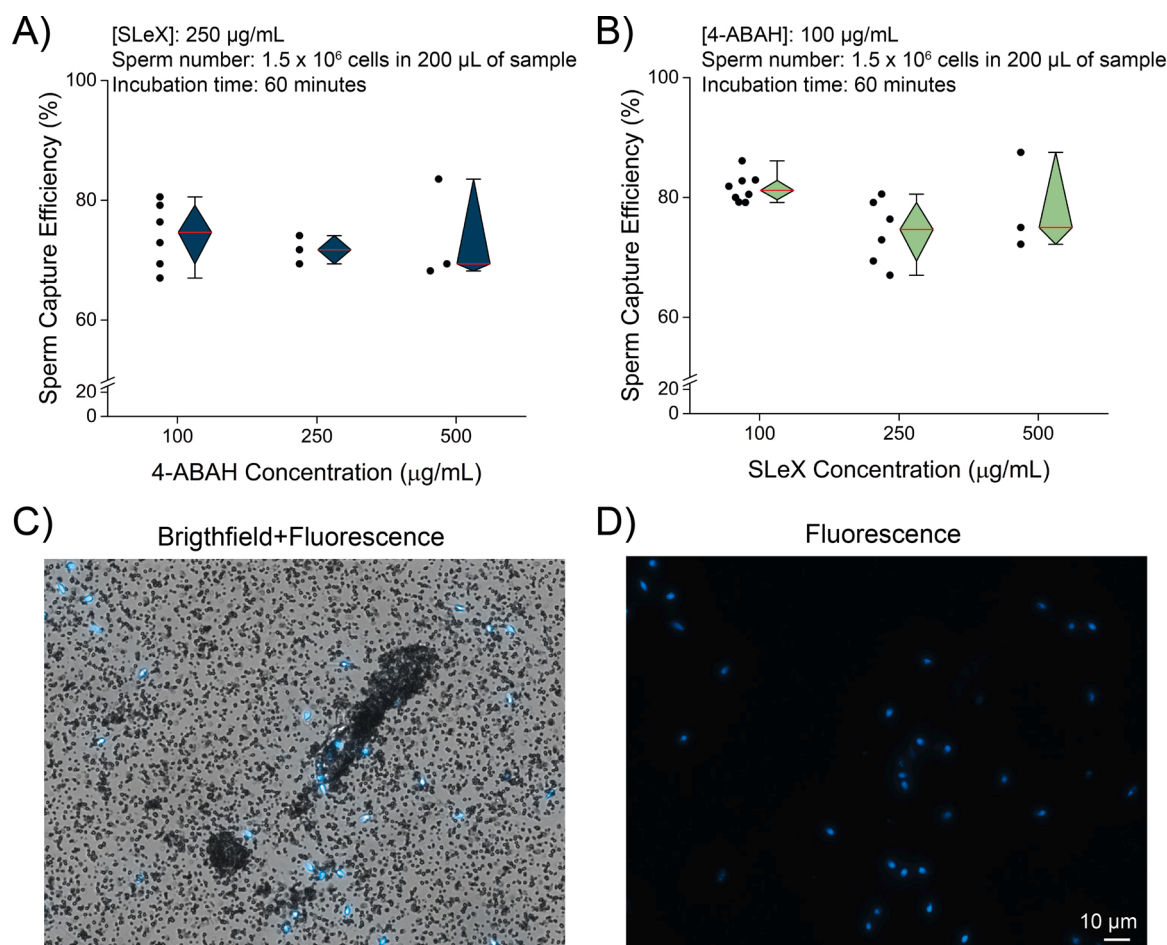


Fig. 2. Evaluation of surface chemistry parameters on magnetic beads. A) Varying agent molecule concentrations (*i.e.*, 4-ABAH) were evaluated. B) Different SLeX concentrations were assessed. In all plots, the sperm capture efficiency (%) was used as the data. C-D) The brightfield and fluorescence images of captured sperm cells were demonstrated. Sperm cells were stained with DAPI, and scale bar represents 10 µm.

(Fig. 2B). Sperm capture efficiencies resulted in $81.6 \pm 2.4\%$ for $100 \mu\text{g/mL}$ of SLeX, $74.3 \pm 5.4\%$ for $250 \mu\text{g/mL}$ of SLeX, and $78.2 \pm 8.2\%$ for $500 \mu\text{g/mL}$ of SLeX. There was no statistical difference observed between all SLeX concentrations ($n = 3-8$, $p > 0.05$) (Fig. 2B and Table S2). By evaluating these two reaction steps, we optimized the experiment with 4-ABA concentration of $100 \mu\text{g/mL}$ and a SLeX concentration of $100 \mu\text{g/mL}$ after the magnetic bead experiments.

During the optimization steps, we also stained the captured sperm cells with DAPI to visualize under a fluorescence microscope (Fig. 2C and D). We mostly observed homogenous distribution of magnetic beads while quantifying sperm on a hemocytometer, and in some cases, magnetic beads were clumped together capturing multiple sperm cells. This is consistent with our previous observation from in-silico experiments [18], where we predicted multiple SLeX binding sites on the sperm surface.

3.2. Characterization of magnetic beads and surface chemistry

Magnetic beads were first characterized with their size parameter using DLS measurements (Fig. 3A). The beads had mostly monodispersed characteristics of a diameter of $942.9 \pm 64.55 \text{ nm}$. We then characterized the surface chemistry by comparing the chemical functionality of bare magnetic beads (NHS-terminated) and modified beads (including SLeX binding) (Fig. 3B). In the FTIR spectrum of bare beads, a characteristic peak at 630 cm^{-1} of Fe-O-Fe was observed. The other peak was Fe-O tensile vibration at 440 cm^{-1} . In addition to iron oxide peaks, succinimide units on the bare beads were clearly visible. Briefly, the asymmetric and symmetric imide stretching vibrations at $\sim 1718-1750 \text{ cm}^{-1}$ and C-C stretching vibration at 1250 cm^{-1} were observed. The tensile vibration of 1453 cm^{-1} C-N was also clearly visible over imide groups. In the SLeX-modified beads, the characteristic peaks of the SLeX were observed at $2850-2925 \text{ cm}^{-1}$ (C-H stretching frequency) and $\sim 1610-1650 \text{ cm}^{-1}$ (C=O stretching frequencies). Besides, the C-O-C etheric tensile vibration appeared at 1066 cm^{-1} . By comparing the FTIR spectra of both beads, it was determined that asymmetric and symmetrical carbonyl stress vibrations caused by NHS groups were reduced. In addition, peaks originating from aliphatic groups were more pronounced. These peaks investigated in the FTIR spectra pointed that SLeX modification on the NHS-activated magnetic beads was performed successfully.

3.3. Evaluating assay procedure

After the surface chemistry was optimized, we determined three

main parameters that could optimize sperm capture: (i) magnetic bead count, (ii) assay incubation time, and (iii) sperm cell number. The bead number was first adjusted by diluting from the stock solution to set counts from 57.5×10^6 to $2,300 \times 10^6$ beads. The incubation time was 60 minutes for this experiment (Fig. 4A). Sperm capture efficiency increased proportionally to the bead count, indicating the increased binding surfaces for sperm capture. The sperm capture efficiencies were calculated as $65.2 \pm 1.8\%$ for 57.5×10^6 beads, $73.7 \pm 1.4\%$ for 165×10^6 beads, $76.8 \pm 3.3\%$ for 230×10^6 beads, $81.6 \pm 2.4\%$ for 575×10^6 beads, $84.5 \pm 3.2\%$ for $1,150 \times 10^6$ beads, and $81.8 \pm 2.7\%$ for $2,300 \times 10^6$ beads. Similarly, the data was represented with Diamond-shaped Box-Whisker plots and analyzed via one-way analysis of variance (ANOVA) followed by Tukey's multiple comparison test. The statistical assessments demonstrated that 57.5×10^6 beads provided the lowest sperm capture efficiency compared to all bead counts; 165×10^6 beads resulted in lower capture efficiency than that of 575×10^6 , $1,150 \times 10^6$, and $2,300 \times 10^6$ beads; 230×10^6 beads provided lower than that of $1,150 \times 10^6$ beads ($n = 3-8$, $p < 0.05$). Further, there was no statistical significance between 575×10^6 , $1,150 \times 10^6$, and $2,300 \times 10^6$ beads ($n = 3-8$, $p > 0.05$). Accordingly, we selected magnetic bead number as 575×10^6 for further experiments.

We then examined the effect of sperm incubation time over capture efficiency, and hence, altered the time slots spanning from 10 minutes to 120 minutes (Fig. 4B). Similarly, we observed the increments in capture efficiency when increasing the incubation time. For instance, we observed the capture efficiencies as $68.2 \pm 4.4\%$ for 10 minutes, $80.3 \pm 2.9\%$ for 20 minutes, $80.7 \pm 2.8\%$ for 30 minutes, $81.6 \pm 2.4\%$ for 60 minutes, and $85.2 \pm 3.4\%$ for 120 minutes. The data was represented with Diamond-shaped Box-Whisker plots and then analyzed through one-way ANOVA with Tukey's multiple comparison test. As a result, we observed that 10 minutes of incubation time resulted in statistically lower sperm capture efficiency than all other incubation time slots ($n = 3-8$, $p < 0.05$), indicating the minimum incubation period for efficient capture. Overall, we defined the incubation period as more than 10 minutes. Accordingly, we performed 30 minutes of incubation for the sperm number evaluation. According to the incubation time results, we further evaluated this parameter with the specificity experiments in the following section.

Lastly, we evaluated the sperm capture performance of magnetic bead platform by applying sperm cells within a range from 1×10^3 to $2,000 \times 10^3$ cells for a 30-minute incubation period (Figs. 4C and S1). We observed that the sperm capture efficiency was dependent on sperm number since we applied a fixed number of magnetic beads. Accordingly, we observed sperm capture efficiencies at highest levels when we

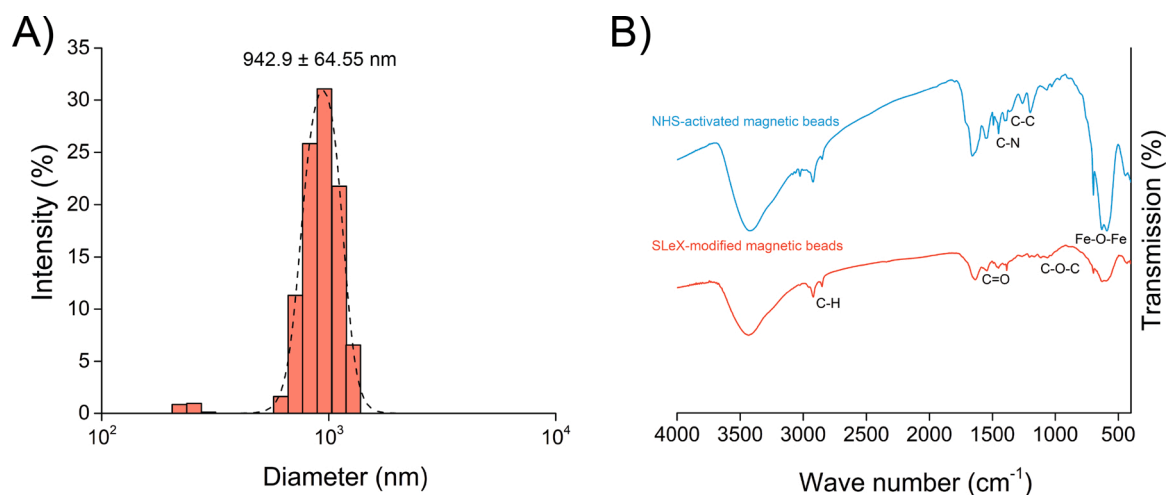


Fig. 3. Characterization of magnetic beads. A) Dimension of magnetic beads was measured using DLS. B) The surface chemistry was evaluated with the FTIR measurements to demonstrate the construction of chemical groups during the functionalization.

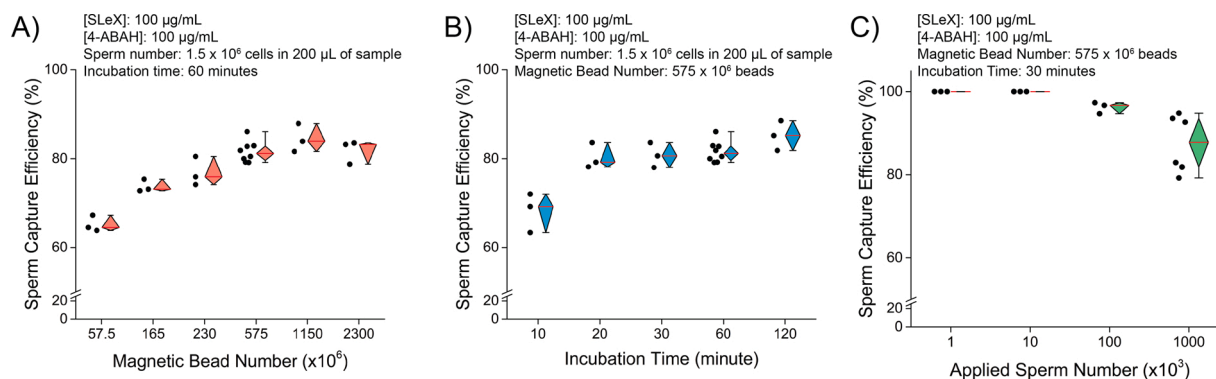


Fig. 4. Evaluating assay procedure. A) Magnetic bead number was assessed within a range from 57.5×10^6 to $2,300 \times 10^6$ beads. B) Sperm incubation time spanning from 10 minutes to 120 minutes was evaluated. C) We also assessed the number of sperm cells applied to the tube, spanning from 1×10^3 to $1,000 \times 10^3$ cells.

applied sperm cells between 1×10^3 and 10×10^3 . The efficiency decreased starting from 100×10^3 of sperm cells, and then saturated at the levels from $1,500 \times 10^3$ to $2,000 \times 10^3$ cells. The data was represented with diamond-shaped Box-Whisker plots, and further analyzed via one-way ANOVA followed by Tukey's multiple comparison test. The lower sperm numbers (1×10^3 to 100×10^3 cells) provided greater efficiency compared to the higher sperm numbers ($1,000 \times 10^3$ to $2,000 \times 10^3$ cells) applied to the tube ($n = 3-6$, $p < 0.05$). There was no statistical significance between the lower sperm numbers ($n = 3$, $p > 0.05$), and similarly there was no difference between the higher sperm numbers ($n = 3-6$, $p > 0.05$). Further, the data derived from sperm numbers of 100×10^3 and $1,000 \times 10^3$ was statistically similar ($n = 3-6$, $p > 0.05$), indicating that we could reach the highest sperm capture performance up to $1,000 \times 10^3$ cells applied to the tube, which might be the highest limit of sperm number observed in the forensic applications.

3.4. Specificity study

After optimizing surface chemistry and assay procedure, we evaluated the specificity performance of the modified beads (all surface chemistry including the SLeX modification). We used two types of epithelial cells: (i) culture vaginal epithelial cells and (ii) buccal epithelial cells. Briefly, we applied a mixture of culture vaginal epithelial cells (6.5×10^3 in 100 μL) and sperm (1.6×10^4 in 100 μL) into the modified bead solution (575×10^6 beads) and incubated for 30 minutes. We observed some non-specific interactions during the procedure (Fig. S2). We considered two possible reasons: (i) the number of beads was too high, and this led to a vortex effect that also dragged vaginal epithelial cells into the collection, and (ii) incubation time was long enough for vaginal epithelial cells to precipitate due to their mass. Therefore, we altered the bead number and the incubation time. As observed in the incubation time experiments (Fig. 4b), the minimum incubation time needed for efficient sperm capture was 10 minutes, and also, the incubation time from 20 minutes to 120 minutes resulted in statistically comparable results. To minimize any non-specific interactions, we performed specificity experiments within an incubation time slot between 10 minutes and 30 minutes. Considering all these parameters to reduce non-specific binding of epithelial cells, we carried out the experiments using a lower number of magnetic beads (287×10^6 beads) and a shorter incubation time (15 minutes), and tested these new parameters with buccal epithelial cells (5×10^3 in 100 μL) and sperm cells (1.6×10^4 in 100 μL) (Fig. 5). Non-modified beads (all chemistry steps were applied, except without SLeX modification) were used as controls, and one-way ANOVA followed by Tukey's multiple comparison test was applied to the data. In both experimental conditions (modified and non-modified beads), a small portion (8.33% to 16.67%) of buccal epithelial cells remained in the tube, and high number of cells were

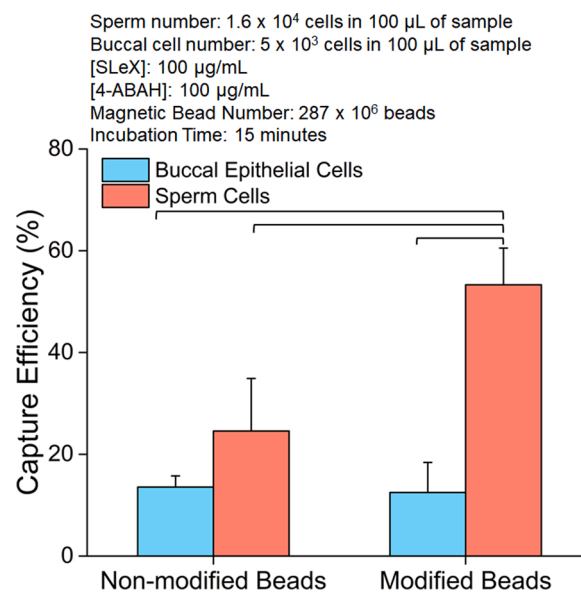


Fig. 5. Specificity experiments. Buccal epithelial cells were used to evaluate specificity features of the modified magnetic beads. In the experiments, non-modified beads were used as controls. Horizontal brackets demonstrate statistically significant differences between groups. Data is represented with average value \pm standard deviation.

removed from the solution. This constant ratio of buccal epithelial cells remained in both situations and this indicated the non-specific interactions during the assay. When non-modified beads were applied, a small portion (24.58%) of sperm cells remained in the tube whereas the modified beads increased the efficiency to 53.3% ($n = 2-3$, $p < 0.05$), indicating that surface chemistry was critical for sperm capture with high efficiency. On the other hand, the specificity parameter was improved with decreasing the bead number and incubation time, yet reduced the sperm capture efficiency compared to the optimized results. Considering the non-specific interactions, different incubation times and various magnetic bead numbers could be evaluated. The other parameters could be optimized accordingly to increase the sperm capture efficiency and specificity at the same time. For example, the addition of detergents, ionic reagents, and/or anti-fouling reagents such as proteins (e.g., bovine serum albumin, casein, glycine, and gelatin), chemical linkers (e.g., thiol-linkers), could be applied as we and others demonstrated earlier [19–25]. In the experiments, we minimized any potential non-specific bindings by altering bead number and reducing the incubation time. Moreover, integrating one of these parameters or reagents could potentially improve the specificity and sensitivity performance.

4. CONCLUSION

The process of separating sperm and epithelial cells has been a problem since the early 1990s, and therefore, any major improvements will have valuable impact on the forensic practice. The earlier efforts present multiple strategies to differentially extract sperm from heterogeneous cell populations. For example, centrifugation was earlier integrated to this process, and it requires multiple centrifugal steps and lengthy processes taking hours of sample manipulations. Fluorescence-activated cell sorting on-chip has provided high specificity due to labelling [26]. However, in addition to the labor-intensive and expensive fluorescence labeling steps (27 minutes for sorting without the labelling procedure), this platform also requires lengthy fabrication steps to develop a complex, multilayer microchip structure that significantly increases the assay cost and efforts for sample preparation. In addition, fluorescence-activated cell sorting on-chip has narrow and shallow channels, which are potentially prone to clogging when a biological sample is applied. As another example to microfluidic approaches, epithelial cells and sperm have been separated under low flow parameters due to their different cellular features, i.e., size [27]. Despite the label-free nature of this method, the processing time (2-3 hours) and fabrication procedure (>10 hours) limit its applicability to the actual workflow in the forensic practice. Di-electrophoresis strategies have been applied to address the sensitivity and specificity challenges, yet this strategy requires considerably more time and processing steps (2–24 hours) than most strategies [28]. On the other hand, researchers have developed an acoustic trapping method performing the differential extraction procedure less than an hour, but the implementation of this method requires many specific optimizations during the measurements with fluorescent beads for frequency scanning that requires specialized training, hence limiting its deployment to the current workflow. In addition to the aforementioned platforms, magnetic bead-based strategies have been used for cell separation and isolation procedures, and forensic labs have benefitted from this strategy [16,17]. Basically, magnetic beads are decorated with antibodies to capture and separate sperm. Despite their utility and easy adaptation to the current workflow, antibody-based strategies have considerable challenges to analyze aged samples (even after a short period of time) due to the structural alterations on membrane receptor proteins of sperm over time. As reported [17], sperm capture efficiency significantly decreases down to ~17% after 10 days. This is a significant impediment and why forensic samples cannot be processed using antibodies to isolate sperm successfully. This also limits their utility and applicability to forensic samples that sit on shelves over multiple years. To circumvent this challenge, we have earlier integrated a specific oligosaccharide sequence (SLeX) with a microfluidic chip, and achieved to differentially extract sperm cells from 15 year old forensic mock samples [18].

In this paper, we (i) integrated the SLeX molecules with a magnetic bead strategy that is a widely used and scalable for cell separation and DNA isolation; (ii) presented that compatibility with a magnetic bead approach is easily integratable with existing downstream commercial forensic lab tools; and (iii) performed less number of sample manipulation steps compared to our earlier work [18]. This hybrid strategy presents specific binding and extraction of sperm cells from epithelial cells in the simulated sexual assault evidence. This process of differential extraction is required for the processing of sexual assault samples entering the standard forensic workflow for further analysis. This method described here provides rapid (25 minutes), accurate, potentially automatable, and easily-integratable option to the current forensic procedures compared to lengthy, expensive, and highly specialized platforms mentioned above. The processing time includes 15 minutes for incubation of a raw, unprocessed sample and another 10 minutes for handling of the sample. Further, the current platform has some manual steps such as adding the sample with cells to the bead solution and removing the supernatant after selective capture of sperm cells. Although these steps are facile and widely performed in a standard

forensic workflow, the current platform could be automated with the integrated platforms such as robotic-arm or cassette-type systems that have only one step of sampling and the other steps are automatically carried out in the device such as RapidHIT ID System (Thermo Fisher). The microfluidic-magnetic bead systems could also have such automatable features using a computer-assisted platform that moves the beads from one step to another for the separation of cells from heterogeneous mixtures [29,30]. These strategies are easy to adapt to our current platform.

We present the core technology with surface functionalization on magnetic beads, and differential extraction of sperm efficiently from bulk solutions. In this study, we modified the beads in bulk solution, and used these beads in the experiments later. The production takes for 20-24 hours of experiential process, including all modification steps and incubation, in which SLeX immobilization takes the most time in the incubation period (~16 to 20 hours). Once the beads are modified, they could be used any time being kept +4 °C. The storage conditions for the prepared beads are in a refrigerator as the commercial magnetic beads are kept until they are used. For the commercial production steps, we envision that the beads would be freeze-dried or incubated with some preservatives such as glycerol to keep their shelf-life for longer periods as applied for the preservation of the other biological materials [31]. Integrating the aforementioned strategies would potentially decrease the assay time and the number of steps, as well as standardize the protocol for all lab settings. Further, we evaluated a broad range of sperm numbers from 10^3 to 10^6 and achieved >81% of capture efficiencies in this study. In our earlier work [18], we presented SLeX reagent was able to capture lower levels of sperm and larger amounts of female vaginal cells in both spiked and mock samples. Based on our earlier experience, this magnetic bead platform with similar chemical structure and same recognition element (i.e., SLeX) would achieve to capture lower levels of sperm in a typical forensic casework. Although we used microcentrifuge tubes (1.5 mL) for processing, the current format can be adapted to a 96-well plate format for multiplexing and a high-throughput operation. In addition, we observed that the capture and isolation of sperm via SLeX molecules did not cause any adverse effects on male DNA collection for downstream analysis [18]. While we apply a similar SLeX-based surface chemistry approach and change a platform strategy from microfluidics to magnetic beads, we expect potential challenges to be addressable with the downstream processing. This bead platform addresses critical technical challenges in forensic labs through easy integration of magnetic bead-type platforms with downstream genomic techniques.

Declaration of Competing Interest

Prof. Utkan Demirci (UD) is a founder of and has an equity interest in: (i) DxNow Inc., a company that is developing microfluidic IVF tools and imaging technologies for point-of-care diagnostic solutions, (ii) Koek Biotech, a company that is developing microfluidic technologies for clinical solutions, (iii) Levitas Inc., a company focusing on developing microfluidic products for sorting rare cells from liquid biopsy in cancer and other diseases, and (iv) Hillel Inc., a company bringing microfluidic cell phone tools to home settings. UD's interests were viewed and managed in accordance with the conflict of interest policies.

Acknowledgements

This work was supported by the National Institute of Justice (2019-NE-BX-0003 and 2020-NE-BX-0004), United States. We would like to thank The Scientific and Technical Research Council of Turkey (TUBITAK) for providing financial support for supporting M.G.K. (2219-International Postdoctoral research fellowship program) during her visit at the BAMM Lab.

Appendix A. Supplementary data

Supplementary material related to this article can be found, in the online version, at doi:<https://doi.org/10.1016/j.fsigen.2020.102451>.

References

- [1] S. Nagrath, L.V. Sequist, S. Maheswaran, D.W. Bell, D. Irimia, L. Ulkus, M.R. Smith, E.L. Kwak, S. Digumarthy, A. Muzikansky, P. Ryan, U.J. Balis, R.G. Tompkins, D. A. Haber, M. Toner, Isolation of rare circulating tumour cells in cancer patients by microchip technology, *Nature* 450 (7173) (2007) 1235–1239, <https://doi.org/10.1038/nature06385>. Dec 20.
- [2] N.G. Durmus, H.C. Tekin, S. Guven, K. Sridhar, A.A. Yildiz, G. Calibasi, I. Ghiran, R. W. Davis, L.M. Steinmetz, U. Demirci, Magnetic levitation of single cells, *Proc. Natl. Acad. Sci. U.S.A.* 112 (28) (2015) E3661–E3668, <https://doi.org/10.1073/pnas.1509250112>. Epub 2015 Jun 29.
- [3] N. Nitta, T. Sugimura, A. Isozaki, H. Mikami, K. Hiraki, S. Sakuma, T. Iino, F. Arai, T. Endo, Y. Fujiwaki, H. Fukuzawa, M. Hase, T. Hayakawa, K. Hiramatsu, Y. Hoshino, M. Inaba, T. Ito, H. Karakawa, Y. Kasai, K. Koizumi, S.W. Lee, C. Lei, M. Li, T. Maeno, S. Matsusaka, D. Murakami, A. Nakagawa, Y. Oguchi, M. Oikawa, T. Ota, K. Shiba, H. Shintaku, Y. Shirasaki, K. Suga, Y. Suzuki, N. Suzuki, Y. Tanaka, H. Tezuka, C. Toyokawa, Y. Yalikun, M. Yamada, M. Yamagishi, T. Yamano, A. Yasumoto, Y. Yatomi, M. Yazawa, D. Di Carlo, Y. Hosokawa, S. Uemura, Y. Ozeki, K. Goda, Intelligent Image-Activated Cell Sorting, *Cell* 175 (Sep(1)) (2018) 266–276.e13, <https://doi.org/10.1016/j.cell.2018.08.028>. Epub 2018 Aug 27.
- [4] B.A. Sutermeister, E.M. Darling, Considerations for high-yield, high-throughput cell enrichment: fluorescence versus magnetic sorting, *Sci. Rep.* 9 (1) (2019) 227, <https://doi.org/10.1038/s41598-018-36698-1>. Jan 18.
- [5] R. Gaudin, N.S. Barteneva, Sorting of small infectious virus particles by flow virometry reveals distinct infectivity profiles, *Nat. Commun.* 6 (2015) 6022, <https://doi.org/10.1038/ncomms7022>. Feb 2.
- [6] F. Inci, Y. Saylan, A.M. Kojouri, M.G. Ogut, A. Denizli, U. Demirci, A disposable microfluidic-integrated hand-held plasmonic platform for protein detection, *Appl. Mater. Today*. 18 (2020) 100478, <https://doi.org/10.1016/j.apmt.2019.100478>. <https://www.sciencedirect.com/science/article/pii/S2352940719305979>.
- [7] W. Asghar, M. Yuksekkaya, H. Shafiee, M. Zhang, M.O. Ozen, F. Inci, M. Kocakulak, U. Demirci, Engineering long shelf life multi-layer biologically active surfaces on microfluidic devices for point of care applications, *Sci. Rep.* 6 (2016) 21163, <https://doi.org/10.1038/srep21163>. <https://www.nature.com/articles/srep21163>.
- [8] S. Tasoglu, H. Cumhur Tekin, F. Inci, S. Knowlton, S.Q. Wang, F. Wang-Johanning, G. Johanning, D. Colevas, U. Demirci, Advances in Nanotechnology and Microfluidics for Human Papillomavirus Diagnostics, *Proc. IEEE*. 103 (2) (2015) 161–178, <https://doi.org/10.1109/JPROC.2014.2384836>. <https://ieeexplore.ieee.org/document/7067030>.
- [9] X.-C. Zhao, L. Wang, J. Sun, B.-W. Jiang, E.-L. Zhang, J. Ye, Isolating Sperm from Cell Mixtures Using Magnetic Beads Coupled with an Anti-PH-20 Antibody for Forensic DNA Analysis, *PLoS One*. 11 (7) (2016) e0159401, <https://doi.org/10.1371/journal.pone.0159401>.
- [10] Y. Xu, J. Xie, R. Chen, Y. Cao, Y. Ping, Q. Xu, W. Hu, D. Wu, L. Gu, H. Zhou, X. Chen, Z. Zhao, J. Zhong, R. Shi, Fluorescence-and magnetic-activated cell sorting strategies to separate spermatozoa involving plural contributors from biological mixtures for human identification, *Sci. Rep.* 6 (2016) 36515, <https://doi.org/10.1038/srep36515>. Nov 18.
- [11] J.V. Norris, M. Evander, K.M. Horsman-Hall, J. Nilsson, T. Laurell, J.P. Landers, Acoustic differential extraction for forensic analysis of sexual assault evidence, *Anal. Chem.* 81 (15) (2009) 6089–6095, <https://doi.org/10.1021/ac900439b>. Aug 1.
- [12] C.T. Sanders, N. Sanchez, J. Ballantyne, D.A. Peterson, Laser microdissection separation of pure spermatozoa from epithelial cells for short tandem repeat analysis*, *J. Forensic Sci.* 51 (2006) 748–757, <https://doi.org/10.1111/j.1556-4029.2006.00180.x>.
- [13] K. Elliott, D.S. Hill, C. Lambert, T.R. Burroughes, P. Gill, Use of laser microdissection greatly improves the recovery of DNA from sperm on microscope slides, *Forensic Sci. Int.* 137 (1) (2003) 28–36, [https://doi.org/10.1016/S0379-0738\(03\)00267-6](https://doi.org/10.1016/S0379-0738(03)00267-6). Oct 14.
- [14] D. Di Martino, G. Giuffrè, N. Staiti, A. Simone, M. Le Donne, L. Saravo, Single sperm cell isolation by laser microdissection, *Forensic Sci. Int.* 146 (Dec 2) (2004), <https://doi.org/10.1016/j.forsciint.2004.09.046>. Suppl:S151-3.
- [15] A.M. Garvin, A. Fischer, J. Schnee-Griese, A. Jelinski, M. Bottinelli, G. Soldati, M. Tubio, V. Castella, N. Monney, N. Malik, M. Madrid, Isolating DNA from sexual assault cases: a comparison of standard methods with a nuclease-based approach, *Investig. Genet.* 3 (1) (2012) 25, <https://doi.org/10.1186/2041-2223-3-25>. Dec 4.
- [16] J. Herr, SpermPaint Optimization and Validation, U.S. Dep. Justice-Cumulative Tech. Prog. Rep., 2007. Grant# 2000-IJ-CX-K013. <https://www.ncjrs.gov/pdffiles1/nij/grants/220289.pdf> (accessed August 21, 2017).
- [17] X.B. Li, Q.S. Wang, Y. Feng, S.H. Ning, Y.Y. Miao, Y.Q. Wang, H.W. Li, Magnetic bead-based separation of sperm from buccal epithelial cells using a monoclonal antibody against MOSPD3, *Int. J. Legal Med.* 128 (Nov(6)) (2014) 905–911, <https://doi.org/10.1007/s00414-014-0983-3>.
- [18] F. Inci, M.O. Ozen, F. Saylan, M. Miansari, D. Cimen, R. Dhara, T. Chinnasamy, M. Yuksekkaya, C. Filippini, D.K. Kumar, S. Calamak, Y. Yesil, N.G. Durmus, G. Duncan, L. Klevan, U. Demirci, A Novel On-Chip Method for Differential Extraction of Sperm in Forensic Cases, *Adv. Sci. (Weinh)* 5 (9) (2018) 1800121, <https://doi.org/10.1002/advs.201800121>. Jun 15.
- [19] F. Inci, C. Filippini, M. Baday, M.O. Ozen, S. Calamak, N.G. Durmus, S. Wang, E. Hanhauser, K.S. Hobbs, F. Juillard, P.P. Kuang, M.L. Vetter, M. Carocci, H. S. Yamamoto, Y. Takagi, U.H. Yildiz, D. Akin, D.R. Wesemann, A. Singhal, P. L. Yang, M.L. Nibert, R.N. Fichorova, D.T.-Y. Lau, T.J. Henrich, K.M. Kaye, S. C. Schachter, D.R. Kuritzkes, L.M. Steinmetz, S.S. Gambhir, R.W. Davis, U. Demirci, Multitarget, quantitative nanoplasmonic electrical field-enhanced resonating device (NE²RD) for diagnostics, *Proc. Natl. Acad. Sci.* 112 (Aug(32)) (2015) E4354–E4363, <https://doi.org/10.1073/pnas.1510824112>. Epub 2015 Jul 20.
- [20] A.R. Statz, R.J. Meagher, A.E. Barron, P.B. Messersmith, New peptidomimetic polymers for antifouling surfaces, *J. Am. Chem. Soc.* 127 (22) (2005) 7972–7973, <https://doi.org/10.1021/ja0522534>. Jun 8.
- [21] Z. Lu, Z. Chen, Y. Guo, Y. Ju, Y. Liu, R. Feng, C. Xiong, C.K. Ober, L. Dong, Flexible Hydrophobic Antifouling Coating with Oriented Nanotopography and Nonleaking Capsaicin, *ACS Appl. Mater. Interfaces*. 10 (Mar(11)) (2018) 9718–9726, <https://doi.org/10.1021/acsami.7b19436>. Epub 2018 Mar 12.
- [22] A. Miodiek, E.M. Regan, N. Bhalla, N.A.E. Hopkins, S.A. Goodchild, P. Estrela, Optimisation and characterisation of anti-fouling ternary SAM layers for impedance-based aptasensors, *Sensors (Basel)*. 15 (10) (2015) 25015–25032, <https://doi.org/10.3390/s151025015>. Sep 29.
- [23] T. Lakshmi Priya, M. Fujimaki, S.C.B. Gopinath, K. Awazu, Y. Horiguchi, Y. Nagasaki, A high-performance waveguide-mode biosensor for detection of factor IX using PEG-based blocking agents to suppress non-specific binding and improve sensitivity, *Analyst*. 138 (10) (2013) 2863–2870, <https://doi.org/10.1039/c3an00298e>. May 21.
- [24] M.V. Riquelme, H. Zhao, V. Srinivasaraghavan, A. Pruden, P. Vikesland, M. Agah, Optimizing blocking of nonspecific bacterial attachment to impedimetric biosensors, *Sens. Bio-Sensing Res.* 8 (2016) 47–54, <https://doi.org/10.1016/j.sbsr.2016.04.003>.
- [25] Y. Nagasaki, Construction of a densely poly(ethylene glycol)-chain-tethered surface and its performance, *Polym. J.* 43 (2011) 949–958, <https://doi.org/10.1038/pj.2011.93>.
- [26] A. Wolff, I.R. Perch-Nielsen, U.D. Larsen, P. Friis, G. Goranovic, C.R. Poulsen, J. P. Kutter, P. Telleman, Integrating advanced functionality in a microfabricated high-throughput fluorescent-activated cell sorter, *Lab Chip*. 3 (Feb(1)) (2003) 22–27, <https://doi.org/10.1039/b209333b>. Epub 2003 Jan 23.
- [27] A.Y. Fu, H.P. Chou, C. Spence, F.H. Arnold, S.R. Quake, An integrated microfabricated cell sorter, *Anal. Chem.* 74 (11) (2002) 2451–2457, <https://doi.org/10.1021/ac0255330>. Jun 1.
- [28] V.R. Williamson, T.M. Laris, R. Romano, M.A. Marciano, Enhanced DNA mixture deconvolution of sexual offense samples using the DEPArray™ system, *Forensic Sci. Int. Genet.* 34 (May) (2018) 265–276, <https://doi.org/10.1016/j.fsigen.2018.03.001>. Epub 2018 Mar 2.
- [29] S. Wang, S. Tasoglu, P.Z. Chen, M. Chen, R. Akbas, S. Wach, C.I. Ozdemir, U. A. Gurkan, F.F. Giguel, D.R. Kuritzkes, U. Demirci, Micro-a-fluidics ELISA for rapid CD4 cell count at the point-of-care, *Sci. Rep.* 4 (2014) 3796, <https://doi.org/10.1038/srep03796>. Jan 22.
- [30] M.O. Ozen, K. Sridhar, M.G. Ogut, A. Shanmugam, A.S. Avadhani, Y. Kobayashi, J. C. Wu, F. Haddad, U. Demirci, Total Microfluidic chip for Multiplexed diagnostics (ToMMx), *Biosens. Bioelectron.* 150 (Feb 15) (2020) 111930, <https://doi.org/10.1016/j.bios.2019.111930>. Epub 2019 Nov 28.
- [31] M. Johnson, Antibody Storage and Antibody Shelf Life, *MATER METHODS* 2 (2012) 120, <https://doi.org/10.13070/mm.en.2.120>. <https://www.labome.com/method/Antibody-Storage-and-Antibody-Shelf-Life.html>.